RSC Advances



This is an *Accepted Manuscript*, which has been through the Royal Society of Chemistry peer review process and has been accepted for publication.

Accepted Manuscripts are published online shortly after acceptance, before technical editing, formatting and proof reading. Using this free service, authors can make their results available to the community, in citable form, before we publish the edited article. This Accepted Manuscript will be replaced by the edited, formatted and paginated article as soon as this is available.

You can find more information about *Accepted Manuscripts* in the **Information for Authors**.

Please note that technical editing may introduce minor changes to the text and/or graphics, which may alter content. The journal's standard <u>Terms & Conditions</u> and the <u>Ethical guidelines</u> still apply. In no event shall the Royal Society of Chemistry be held responsible for any errors or omissions in this *Accepted Manuscript* or any consequences arising from the use of any information it contains.



- 1 Synthesis and application of polypyrrole coated tenorite nanoparticles (PPy@TN) for the
- 2 removal of anionic food dye 'Tartrazine' and divalent metallic ions viz. Pb(II), Cd(II),
- 3 Zn(II), Co(II), Mn(II) from synthetic wastewater
- 4 **Varsha Srivastava**^{a*}, Philipp Madyannik^a ,Y.C.Sharma^b, Mika Sillanpää^a
- ^aLaboratory of Green Chemistry, Faculty of Technology, Lappeenranta University of
- 6 Technology, Sammonkatu 12, FI-50130, Mikkeli, Finland.
- 7 ^bDepartment of Chemistry, Indian Institute of Technology, Banaras Hindu University,
- 8 Varanasi 221005, India.

10

11

12

- **Corresponding author: Dr. Varsha Srivastava
- 14 Laboratory of Green Chemistry,
- 15 Faculty of Technology, Lappeenranta University of Technology,
- 16 Sammonkatu 12,FI-50130, Mikkeli, Finland

17

- 18 Email id: <u>varsha06bhu@gmail.com</u>
- 19 *varsha.srivastava@lut.fi*
- 20 *Contact no:* +358414712348

21

1	Highlights
---	------------

- Polypyrrole coated tenorite nanoparticles with brick like morphology were successfully
 synthesized.
- Synthesized nanoparticles were found to be very efficient for the removal of an anionic food dye 'Tartrazine'.
- 6 Acidic medium was found to be favorable for tartrazine adsorption.
- - Endothermic nature was observed for tartrazine removal.
- Exhausted (dye loaded) nanoparticles acted as an efficient adsorbent for the removal of
 divalent metallic ions.

- 1 Synthesis and application of polypyrrole coated tenorite nanoparticles (PPy@TN) for the
- 2 removal of anionic food dye 'Tartrazine' and divalent metallic ions viz. Pb(II),Cd(II),
- 3 Zn(II), Co(II), Mn(II) from synthetic wastewater
- 4 **Varsha Srivastava**^{a*}, Philipp Madyannik^a, Y.C.Sharma^b, Mika Sillanpää^a
- ^aLaboratory of Green Chemistry, Faculty of Technology, Lappeenranta University of
- 6 Technology, Sammonkatu 12, FI-50130, Mikkeli, Finland.
- 7 bDepartment of Chemistry, Indian Institute of Technology, Banaras Hindu University,
- 8 Varanasi 221005, India.
- 9 Abstract:
- Present study deals with the synthesis of polypyrrole coated tenorite nanoparticles. Synthesized 10 nanoparticles were characterized by XRD, TEM, SEM and EDS. TEM images showed the 11 formation of nanoparticles with 26-30 nm diameter. BET surface area of nanoparticles was 12 determined to be 425 m²/g while the pore diameter of nanoparticles was found to be 3.57 nm 13 which showed the formation of mesoporous nanoparticles. pH_{zpc} of nanoparticles was determined 14 to be 4.4. The removal efficiency of synthesized nanoparticles for an anionic food dye 15 'Tartrazine' was investigated. Decreased removal was observed, when dye concentration was 16 increased from 100 to 200 mg/L. It was observed that acidic medium was favorable for tartrazine 17 removal. A thermodynamic study suggested the endothermic nature of Tartrazine adsorption. The 18 value of E_a for present system was found to be 26.97 kJ/mol. The best suitable kinetic model was 19 well explained by the pseudo second order model. Langmuir adsorption capacity was measured to 20 be 42.50 mg/g. Exhausted (dye loaded) nanoparticles were used as an efficient adsorbent for the 21 removal of divalent metallic ions viz. Pb(II), Cd(II), Co(II), Mn(II), Zn(II) and were found to be 22 efficient for the removal of metallic species from the single solute system as well as multi-solute 23

- system. This study reveals that polypyrrole coated tenorite nanoparticles are very efficient for dye
- 2 removal and dye loaded exhausted adsorbent is equally good for metal removal because tartrazine
- 3 loading on nanoparticles makes its surface suitable for metal interaction. Thus, synthesized
- 4 nanoparticles can prove to be a good candidate for the treatment of dye and metals bearing
- 5 wastewater.
- 6 **Keywords**: Pyrrole, nanoparticles, anionic dye, metal removal, isotherm study.

7 1.0 Introduction

- 8 Many industries such as pharmaceutical, textile, plastics, leather, cosmetic, printing, paper, rubber
- 9 and food industries often use a variety of dyes in different processes and usually discharge a large
- amount of dye containing waste into the aquatic environment^{1,2}. Most of the dyes are harmful to
- fauna and flora³. Dyes may pose carcinogenic and mutagenic effect⁴. Further, dye containing
- effluents may affect aquatic environment by interrupting transmission of sunlight into the aqueous
- streams^{3,5}. Among various dyes, tartrazine is commonly used in a variety of food materials as
- coloring agent ⁶. Tartrazine is also used in shells of medicinal capsules, cosmetics, vitamins and
- syrups^{7,8} Tartrazine $(C_{16}H_9N_4Na_3O_9S_2)$ is an anionic dye which releases anions in aqueous
- 16 medium $(Fig.1)^9$.

17 Fig.1

- 18 Though, tartrazine is used in variety of food materials, but its higher amount can pose mutagenic
- and carcinogenic effects^{5,8,10}. Other health problems which can arise due to excess inhalation of
- 20 tartrazine are asthma, migraine, itching, hypersensitivity, thyroid cancer, blurred vision and skin
- eczema. Due to the toxic nature of dyes, much attention should be paid for proper treatment of dye
- bearing wastewater before being discharged into the water stream. Several techniques viz.
- 23 Precipitation, ozonation, reverse osmosis, ion-exchange, membrane filtration, electrochemical

- oxidation, coagulation, flocculation and adsorption have been developed for the treatment of dye-
- 2 containing effluents^{1,6,11}. However, most of these technologies are expensive and not highly
- 3 efficient for the treatment of a wide range of dye containing wastewater.
- 4 Among these methods, adsorption technique has been considered to be cost effective and efficient
- 5 technique for the treatment of dye loaded wastewater^{3,12,13}. Variety of adsorbents have been
- 6 discovered and used for the treatment of dye laden wastewater^{7,14,15}. Among them, activated
- 7 carbon is the most widely used adsorbent to remove different kinds of dyes from wastewater
- 8 because of its high adsorption capacity, but at the same time its high cost has always inspired the
- 9 scientists to discover new adsorbent materials. Recently, nanosized materials have emerged as a
- strong competitor of conventional adsorbent materials due to their unique properties such as the
- large surface area to volume ratio, chemical stability, etc. and have attracted attention of several
- researchers to develop varieties of nanomaterials for water treatment process 16,17. Properties of
- nanomaterial can be further improvised by chemical modification according to pollutant species
- which makes it a strong candidate for treatment of both organic and inorganic pollutants 18,19.
- 15 Polypyrrole modified adsorbent materials were found to be very efficient in removal of
- nitrophenols, reactive blue 19, alizarin red-S, alizarin yellow GG etc. ^{20,21}. In the present study,
- polypyrrole coated tenorite (PPy@TN) nanoparticles were synthesized and characterized by
- different techniques. PPv@TN nanoparticles were used for the removal of an anionic food dye
- 19 'Tartrazine dye' (TZ) from synthetic wastewater. The effect of various important parameters was
- 20 investigated and optimum conditions for maximum removal were determined. After dye
- adsorption, tartrazine loaded nanoparticles (TZ-PPy@TN) were used as adsorbent material for the
- treatment of divalent metallic ions from synthetic wastewater.

2. Materials and method

- 1 2.1. Synthesis of polypyrrole coated tenorite (PPy@TN) nanoparticles
- 2 Synthesis of PPy@TN can be divided into two parts (a) Synthesis of tenorite nanoparticles (TN)
- and (b) modification of tenorite nanoparticles with polypyrrole (PPy@TN).
- 4 For the synthesis of tenorite nanoparticles, the copper nitrate solution was precipitated by adding
- 5 ammonia solution drop by drop into 0.5M copper nitrate solution. After precipitation, precipitate
- 6 (Cu(OH)₂) was separated by centrifugation and washed several times with ultrapure water. After
- 7 proper washing, the precipitate was dried in hot air oven at 60 °C. Dried precipitate was then
- 8 calcined at 400° C ($\pm 0.2^{\circ}$ C) for 2 h in the Muffle furnace (NABERTHERM B-170) by
- 9 maintaining heating rate of 5⁰C/min to get tenorite nanoparticles.
- 10 (b) For synthesis of PPy@TN nanoparticles, 5 g of tenorite nanoparticles were sonicated in 150
- 11 ml of ultrapure water and then 5 ml of pyrrole was added into this solution and stirred for 15 min.
- After stirring, FeCl₃ solution (oxidizing agent) was added drop by drop into this mixture solution
- and again stirred for 5 h on a magnetic stirrer at room temperature. The colour of solution changed
- from brown to black on adding FeCl₃. After a sufficient contact time, polypyrrole coated tenorite
- nanoparticles were separated from the solution by centrifugation at 5000 RPM for 15 min. and
- multistep washing was carried out for the removal of another product (FeCl₂) which was formed
- during the reaction of pyrrole and FeCl₃. Separated PPy@TN nanoparticles were dried and
- 18 grounded in tube mill and sieved to remove lumps of particles formed during the drying process.
- 19 Tenorite nanoparticles, PPy@TN and dye loaded nanoparticles (TZ-PPy@TN) were characterized
- by transmission electron microscopy(TEM), X-ray diffraction(XRD), energy-dispersive X-ray
- spectroscopy (EDS) and scanning electron microscopy(SEM). PPy@TN nanoparticles were used
- 22 for the removal of tartrazine dye from synthetic wastewater. Dye loaded nanoparticles were used
- 23 for the treatment of divalent metallic ions from synthetic wastewater. XRD patterns of

- nanoparticles were recorded on a PANALYTICAL X-ray diffractometer using Co Kα radiation (λ 1 = 1.790307A⁰) operated at 40 kV and 40 mA in the 20 range of 15–100⁰. The particle size and 2 morphology of the samples were determined by using TEM images taken with a Hitachi H-7600 3 4 TEM with an acceleration voltage of 200 kV. The surface morphology was studied by SEM analysis, using the Hitachi S-4800 system with an acceleration voltage of 20 and 30 kV. 5 Elemental analysis of nanoparticles was examined by EDS. FTIR images of tenorite nanoparticles 6 and PPY@TN nanoparticles were recorded in the range of 400 to 4000cm⁻¹ by using (ATR-FTIR, 7 Bruker Vertex 70) model) to investigate the changes in tenorite nanoparticles due to modification 8 with polypyrrole nanoparticles. For determination of BET surface area, nitrogen adsorption— 9 desorption measurements were conducted at 77 K with a Quantachrome instrument. The powders 10 were degassed in vacuum at 150 °C for 24 h prior to the measurement. pH_{zpc} of nanoparticles was 11 determined by earlier reported method²². In brief, 0.01M NaCl solutions of different pH ranging 12 from 2 to 12 were prepared. 0.2 0g of nanoparticles were placed in NaCl solution of different pH 13 and solution was kept for 48 h and then nanoparticles were separated from NaCl solution and the 14 pH of the solution was measured. A graph between initial pH and final pH was plotted and the 15 intersection of initial and final pH was recorded as pH_{zpc} of adsorbent. 16 2.2. Treatment of tartrazine bearing synthetic wastewater 17
- Removal study of tartrazine (TZ) from synthetic wastewater was performed in a batch process to optimize various important parameters such as contact time, concentration, dose, pH and temperature. Stock solution (1000 mg/L) of TZ was prepared by dissolving required amount of TZ in ultrapure water. TZ solution with different concentration ranges (100 to 200 mg/L) were prepared by diluting the stock solution. pH of TZ solutions was adjusted by adding 0.1 M HCl/NaOH solution. Adsorption experiments were conducted with different dye concentration

- 1 (100-200 mg/L), dosage (1 to 10 g/L), temperature (293-323 K) and pH (2.0 to 12.0) to
- 2 investigate the effect of each variable on TZ removal from synthetic wastewater. For batch
- 3 experiments, 1g/L of PPy@TN nanoparticle was added into dye solution and agitated at room
- 4 temperature in a temperature controlled shaker. Treated dye solutions were collected at different
- 5 time intervals to determine the equilibrium time. Nanoparticles were separated from the dye
- 6 solution by centrifugation at 4000 rpm for 10 min and the absorbance of supernatant solution was
- 7 recorded by UV-visible spectrophotometer at λ_{max} 430 nm for residual dye concentration⁸. The
- 8 removal (%) of dye and the amount of dye adsorbed were calculated by following equations.
- 9 Removal of dye (%) = $\left(\frac{C_i C_e}{C_0}\right) * 100$ (1)

$$q_e = \left(\frac{C_i - C_e}{W}\right) * V \tag{2}$$

- 11 Where C_i(mg.L⁻¹) and C_e(mg.L⁻¹) are the initial and equilibrium concentrations of dye
- respectively. q_e(mg.g⁻¹) is the amount adsorbed on per unit mass of the adsorbent at equilibrium,
- W is the mass of adsorbent (g) and V(L) is the volume of solution. Dye loaded nanoparticles were
- further used as adsorbent for the removal of metallic ions viz. Pb(II), Cd(II), Co(II), Mn(II), Zn(II)
- from synthetic wastewater. For this study, the single solute solution of four different concentration
- ranges viz. 75, 100, 125 and 150 mg/L were prepared by adding the appropriate amounts of their
- salt into ultrapure water. Multisolute metal solution of 100 mg/L was also prepared to observe the
- adsorption capacity of nanoparticle for different metals in a multisolute system. The residual
- 19 concentration of metal was determined by ICP-OES spectrometer.

3. Result and discussions

20

21 3.1. Characterization of nanoparticles

1 XRD analysis of tenorite nanoparticle, polypyrrole coated tenorite nanoparticles (PPv@TN) and 2 tartrazine loaded nanoparticles (TZ-PPv@ TN) are shown in Fig.2. In Fig 2(a), all peaks correspond to the tenorite phase of CuO and all the diffraction peaks can be indexed to tenorite 3 4 phase of CuO which is in good agreement with the reference data (ICPDS data 98-001-6025). It is clear from XRD of polypyrrole coated tenorite nanoparticles that polypyrrole has modified the 5 tenorite nanoparticles and new peaks appear in the modified sample due to polypyrrole reaction 6 7 (Fig 2b). However, intensity of characteristic peaks of nano tenorite is very low in the coated sample. According to EDS analysis of tenorite nanoparticles, the Cu/O atomic ratio (Cu=51.02%; 8 O=48.98%) was 1.04(Fig. 2a-1). Elemental composition of PPy@TN nanoparticle is different from 9 tenorite nanoparticles, which shows the modification of tenorite nanoparticles (Fig 2b-1). Further, 10 elemental composition of TZ-PPy@TN nanoparticles shows the presence of other elements like N 11

and S which is due to dye loading (Fig 2c-1). TEM images of nano tenorite, PPy@TN and TZ-

14 Fig. 2

PPy@TN nanoparticles are shown in Fig. 3.

12

- 15 Fig.3
- 16 Fig.4
- The TEM image of nano tenorite shows the formation of well dispersed hexagonal and spherical nanoparticles with mean diameter~23-45 nm. After polypyrrole coating, some tube like and brick like structures appeared having diameter in the range of ~26-30 nm. In TZ-PPy@TN nanoparticles, almost all particles have similar morphology like a small tube structure (~5-11 nm). Further, surface morphology was investigated by SEM. SEM images of nano tenorite and PPY@TN and TZ-PPy@TN nanoparticles are given in Fig 4. SEM of nano tenorite also shows

- that the particle morphology is spherical and hexagonal (Fig.4a,b). SEM images of PPY@TN
- 2 nanoparticles showed different morphology, which indicates that polypyrrole completely modified
- 3 the surface of tenorite nanoparticles (Fig.4 c,d). Highly agglomerated particles can be seen in TZ-
- 4 PPY@TN nanoparticles (Fig. 4 e,f). FTIR of tenorite nanoparticle, PPy @TN and TZ-PPy@ TN
- 5 further is shown in Fig.S1 (In supplementary material). FTIR results clearly indicates that
- 6 polypyrrole totally changed surface properties of tenorite nanoparticles (In supplementary
- 7 material, section S1).
- 8 Fig. 5
- 9 N₂ adsorption and desorption isotherms of nanoparticles are shown in Fig 5. BET surface area of
- synthesized nanoparticles was determined to be 425 m²/g, while pore volume and pore diameter
- were 0.38 cc/g and 3.57 nm respectively. Value of pore diameter suggested the formation of
- mesoporous nanoparticles.
- BET surface area of tenorite nanoparticles and TZ-PPY@TN nanoparticles were calculated with
- their N₂ adsorption and desorption isotherms (In supplementary material Fig.S2a and Fig.S2b).
- 15 BET surface area, pore volume and pore diameter of tenorite nanoparticles were calculated to be
- 16 6.56m²/g, 0.002cc/g and 1.107nm respectively while BET surface area of TZ-PPY@TN were
- determined to be 51.49m²/g. Decreased surface area of TZ-PPY@TN in comparison of PPY@TN
- nanoparticles is due to loading of dye molecules on PPY@TN nanoparticles. Pore volume for
- 19 TZ-PPY@TN was recorded to be 0.013cc/g while pore diameter was found to be 0.99nm.

20 3.2. Adsorption studies

- 21 *3.2.1. Effect of contact time and initial dye concentration*
- The contact time is the most important design parameter. The appropriate contact time between
- adsorbent and adsorbate during the adsorption process is necessary to achieve maximum removal

- 1 of pollutant species. In this view, dve solution was agitated with adsorbent for different time
- intervals from 15 min to 420 min. 2

3 Fig. 6

4

5

6

8

9

10

11

12

13

14

15

16

17

18

19

20

21

- It was observed that initial removal rate is very rapid and approximately 87% (± 0.01) of dye were removed within 15 min. Removal of dye rapidly increased up to 180 min and thereafter up to 300 min of contact time, we get approximately the same result and further no change in removal 7 percentage was observed upto 420 min. This behavior is due to availability of plenty of adsorption sites at the initial stage. After equilibrium time (300 min), there is no change in the removal of dye so 300 min contact time was selected for all other experimental setup. To see the effect of initial concentration on the removal of dye, batch experiments with different dye concentration ranges were carried out at equilibrium time and the plot of adsorption capacity (q_e)/removal (%) versus different TZ concentration is shown in Fig.6. Removal of dye decreased on increasing dye concentration. At lower initial concentration, excess adsorption sites are available for dye molecules, but for higher concentration of dye, the ratio of adsorbent sites are reduced in comparison to available dye molecules and all the binding sites easily get saturated due to the higher concentration of dye molecules in the solution resulting in the decreased removal at higher concentration. Further, the residual dye concentration is higher for higher dye concentrations. At a fixed nanoparticle dose, the amount of dye adsorbed increased from 29.28 to 41.27 mg/g(± 0.01) by increasing concentration of dve solution from 100 to 200 mg/L. In case of lower concentration most of the adsorption sites remain unoccupied due to less number of dye molecules while for higher concentration most of the binding sites were occupied by a dye molecule resulting in higher adsorption capacity in comparison to lower concentration.
- 3.2.2. Effect of pH on removal of tartrazine 23

- 1 Solution pH is an important factor which is responsible for the adsorbent surface charge and the
- 2 degree of ionization. Effect of solution pH on removal of TZ was assessed by varying pH in the
- range of 2.0 to 12 by keeping the other experimental conditions constant (100 mg/L; 200 rpm; 293
- 4 K; 0.05 g/15ml dose, contact time 300 min). The effect of solution pH on removal of TZ is shown
- 5 in Fig.7a. It was observed that the removal of dye was higher in acidic medium in comparison to
- 6 alkaline medium. Similar findings were also reported by Mittal et al.(2007)⁶. Removal decreased
- 7 from 99.28 to 73.88%(±0.01) on increasing pH from 2.0 to 12.0. pH_{zpc} of PPy@TN was recorded
- 8 to be 4.4 (Fig. 7b). When the pH of solution is lower than pH_{zpc} of adsorbent, surface will be
- 9 positively charged but as pH goes above pH_{zpc}, number of negatively charged adsorbent surface
- sites increases. In aqueous solution, tartrazine releases sodium ions and sulfonate anions. In acidic
- medium, due to positively charged surface sulfonate anions can be easily adsorbed.
- Fig. 7(a)
- 13 Further, in acidic medium, high degree of surface protonation favors electrostatic attraction
- between positively charged adsorbent surfaces and negatively charged anionic sulfonate groups.
- In contrast, at higher pH values (pH > pH_{zpc}), the adsorbent surface becomes more negatively
- 16 charged.
- 17 Fig. 7(b)
- 18 In alkaline medium, excess amount of -OH ions compete with the negatively charged anionic
- 19 species and electrostatic repulsion between the anionic species and the negatively charged surface
- sites is increased, resulting in the decreased removal of TZ.
- 3.2.3. Effect of adsorbent dose on removal of TZ dye
- The adsorbent dose is an important parameter which can affect the removal of pollutants. The
- effect of adsorbent dose on removal of TZ was investigated by adding different amounts of dose

- (1 to 10 g/L) into dve solution of 100 mg/L and agitating at 200 rpm for 300 min. After 1 2 equilibrium time, the TZ solution was-separated from adsorbent by centrifugation and the residual concentration in the supernatant dye solution was analyzed. The plot of TZ removal (%) versus 3 4 dose (g/L) is shown in Fig.8. The removal of TZ increased rapidly from 74.50 to 98.89 $\%(\pm 0.02)$ by increasing adsorbent dose from 1 g/L to 3.3 g/L and after that there was not any significant 5 change in removal percentage of TZ. Approximately similar result was observed even at higher 6 adsorbent dose. This behavior is obvious because on increasing adsorbent dose initially, removal 7 increased due to the availability of more active sites for a fixed amount of dye concentration. 8
- 9 However, adsorption capacity (mg/g) decreased with further increasing of adsorbent dose due to 10 unsaturated surface at higher adsorbent dose for a particular concentration. Higher adsorbent
- dosage may also cause aggregation of adsorption sites which can decrease total available
- adsorbent surface for adsorbate interaction²³.
- 13 **Fig.8**

4. Kinetic modelling of tartrazine removal process

- 15 The study of adsorption kinetics is necessary for understanding the mechanism of adsorption process and also gives an idea about the rate at which a pollutant species is removed from aqueous 16 solutions²⁴. Several processes may be involved in the removal of any pollutant species such as 17 pore diffusion, film diffusion and intraparticle diffusion. In order to explain the adsorption 18 mechanism, kinetic adsorption data were analyzed by using different kinetic models viz. pseudo 19 first-order model, pseudo-second-order model, Intraparticle diffusion, Boyd model and Bangham 20 21 model. The kinetic data were collected for various initial dye concentrations by keeping other experimental parameters constant. 22
- 23 4.1. Pseudo first order and Pseudo second order model

- 1 The values of pseudo first order and second order kinetic model were calculated from the
- 2 following equations²⁵:

3 Pseudo first order:
$$\log(q_e - q_t) = \log q_e - \frac{k_1}{2.303}t$$
 (3)

4 Pseudo second order model:
$$\frac{t}{q_t} = \frac{1}{k_2 q_e^2} + \frac{1}{q_e} t$$
 (4)

5
$$h = k_2 q_e^2$$
 (5)

- Where $k_1 \, (min^{-1})$ and $k_2 \, (g \, mg^{-1} \, min^{-1})$ are the rate constants of pseudo-first and pseudo-second
- order models respectively. h is known as the initial adsorption rate $(g mg^{-1}min^{-1})$. $q_t(mg/g)$ and
- 8 q_e(mg/g) are the amounts of dye adsorbed at time t and equilibrium respectively. t is the contact
- 9 time(min). The slope and intercept of the plot of log $(q_e q_t)$ against t gives the value of k_1 and q_e
- 10 respectively, while the slope and intercept of the plot of t/q_t versus t gives the value of pseudo-
- second-order rate constant (k₂) and the equilibrium adsorption capacity (q_e) respectively. The
- values of different kinetic parameters at different concentrations are shown in Table 1.
- 13 Fig.9.
- It is clear from Fig. 9a that the plots of $log (q_e-q_t)$ versus t for pseudo first order kinetic model
- does not show good results while the plots of t/q_t versus t (Fig. 9b) gives a straight line for all the
- selected dye concentrations which shows the applicability of the pseudo-second order equation for
- 17 TZ adsorption. Further, it is clear from Table 1 that qe values calculated from pseudo-second-
- order model is rather comparable with experimental q_e in comparison to pseudo first order model.
- 19 Calculated value of q_e is not consistent with experimental q_e values for pseudo first order model
- which indicates the suitability of the pseudo-second-order model. The corresponding R^2 value
- 21 was greater for pseudo second order model in comparison to pseudo-first-order kinetic model
- 22 which also supports the suitability of pseudo second order kinetic model. Fast removal of TZ from
- 23 adsorbate solution suggested that most part of the adsorbate removed by interaction of exterior

- surface of adsorbent while later adsorption may be due to involvement of other process like
- 2 Intraparticle and pore diffusion mechanism.
- 3 *4.2. Intraparticle diffusion model*
- 4 The possibility of intraparticle diffusion was also investigated to identify the rate determining step
- 5 by applying Weber Morris intraparticle diffusion model on kinetic data. Intraparticle diffusion
- 6 model can be expressed as follows²⁶:
- 7 $q_t = k_{id}t^{0.5} + C$ (6)
- 8 Where q_t, k_{id} and C are the amount of adsorbed dye onto adsorbent (mg/g) at time t, intraparticle
- 9 diffusion rate constant and intercept (mg/g) respectively.
- 10 **Table 1.**
- 11 Fig.10.

The values of K_{id} and C were calculated from the slope and intercept of plot q_t versus $t^{0.5}$. The 12 intercept 'C' which is proportional to boundry layer thickness, gives an idea about the thickness of 13 the boundary layer. In case of the larger intercept, the boundary layer effect will be greater. 14 Intraparticle diffusion usually starts when surface of adsorbent get saturated with adsorbate 15 molecules. The value of K_{id} increased with increasing dye concentration due to driving 16 17 force.(Table.1) Intra-particle diffusion plot for all selected concentration was found to be linear with good correlation coefficient (Fig. 10a) which indicates the possibility of intraparticle 18 19 diffusion of dye molecule. According to this model if the linearized curve passes through the 20 origin, intraparticle diffusion plot will be the rate controlling step, but in present case, the lines of plot do not pass through the origin it shows that the intraparticle diffusion is not the only rate 21 limiting factor in case of TZ removal by PPy@TN nanoparticles²³. Further, R² vales determined 22

for all selected concentration showed the feasibility of Intraparticle diffusion model.

- 1 4.3. Boyd model
- 2 Removal of adsorbate molecules can also be assessed by film diffusion, so to check the possibility
- 3 of film diffusion, Boyd model was also applied on kinetic data. It can be expressed by following
- 4 equations²⁷:

$$5 F = \left(1 - \frac{6}{\pi^2}\right) exp(-B_t) (7)$$

6
$$B_t = -0.4977 - \ln(1 - F)$$
 (8)

$$7 F = q_t/q_e (9)$$

- 8 B_t is a mathematical function of F, while F is the fraction of dye molecule adsorbed at any time q_t
- 9 (mg/g) and dye molecule adsorbed at equilibrium q_e (mg/g). The plots of B_t vs. t at different initial
- 10 concentrations are shown in Fig. 10b. The value of B (min⁻¹) was calculated from the slope of the
- Boyd plot 'B_t versus t'. The linearity of Boyd plot gives an idea to distinguish between
- 12 Intraparticle diffusion and film diffusion. It is clear from Boyd plot that linear plots are not
- passing through the origin, which indicate that adsorption process is governed by film diffusion
- but it is not only the rate controlling step. Value of D_i (m²/min), diffusion constant can be
- 15 calculated from following equation:

$$\mathbf{B} = \frac{\pi^2 D_i}{r^2} \tag{10}$$

- Where 'r' is the radius of adsorbent particles.
- 18 4.5. Bangham's equation (Pore diffusion model)
- In some cases pore diffusion may be the only rate controlling step. To check this possibility in
- present system, Bangham's equation was applied on kinetic data by using following equation ^{28,29}:

- $1 \quad \log\left[\log\left(\frac{c_0}{c_0 a_t m}\right)\right] = \log\left(\frac{k_0 m}{2.303 V}\right) + \alpha \log(t) \tag{11}$
- Where $\alpha(<1)$ and k_0 are the Bangham constants. q_t (mg/g) is the dye amount adsorbed at time t,
- 3 C_o is the initial dye concentration (mg/L), V is the volume of dye solution(ml), m is the weight of
- adsorbent (g/L). Values of Bangham parameters, α and k_0 were obtained from the slopes and
- intercepts of plot $\log \left[\log \left(C_0/(C_0 q_t m)\right)\right]$ versus $\log t$ (Fig. 10c). The values of α and k_0 are given
- 6 in Table 2. The plot was found to be linear for all selected concentration ranges with good
- 7 correlation coefficient (>0.9) indicating pore diffusion is the only rate controlling step.
- 8 5. Effect of temperature and thermodynamic study
- 9 Usually dye industries release effluents at different temperatures^{30.} The temperature has
- 10 significant effect on the adsorption process, so it is necessary to investigate the effect of
- 11 temperature on removal of TZ.
- 12 Fig.10
- To study this effect, TZ solutions of different concentrations viz. 100,125,150,175 and 200 mg/L
- were agitated with adsorbent at four different temperatures 293, 303, 313 and 323K up to
- equilibrium. Fig.10 depicts the effect of temperature on the removal of TZ from synthetic
- wastewater. Increased dye removal on increasing solution temperature indicates the endothermic
- 17 nature of removal process. The reason of increased removal at higher temperature may be due to
- the increased mobility of adsorbate molecules and also due to pore enlargement which exposes
- more surface sites for adsorbate interaction.
- 20 Thermodynamic parameters provide important information about the mechanism of adsorbate
- removal. Various thermodynamic parameters viz. change in Gibbs free energy (ΔG^{o}), change in
- enthalpy (ΔH^{o}) and change in entropy (ΔS^{o}) were calculated by the following equations²⁵:

$$\Delta G^{0} = -RT \ln K_{c} \tag{12}$$

$$1 \qquad \Delta H^{\circ} = R \left(\frac{T_2 T_1}{T_2 - T_1} \right) \ln \frac{kc_2}{kc_1} \tag{13}$$

$$2 \qquad \Delta S^{\circ} = \frac{\Delta H^{\circ} - \Delta G^{\circ}}{T} \tag{14}$$

Where ΔG^{0} is the Gibbs free energy change (kJ/mol), R is the universal gas constant (8.314 J 3 mol⁻¹ K⁻¹), T is absolute temperature (K) and K_c is the distribution coefficient, C_e is the 4 equilibrium concentration of TZ dyes, qe is the amount of TZ dyes adsorbed per unit weight of 5 nanoparticles at equilibrium. The value of ΔG^{0} was determined to be -9.06, -11.04, -12.77 and -6 16.07 at 293, 303, 313 and 323K respectively. The negative value of ΔG° at all selected 7 temperatures, shows spontaneous nature of adsorption process and confirm the feasibility of TZ 8 adsorption on PPY@TN nanoparticles. The Gibbs free energy change for physisorption is 9 between -20 and 0 kJ/mol while for chemisorption it is in a range of -80 to 400 kJ/mol^{23,31}. The 10 values of ΔG° obtained for present system are within the ranges of the physisorption mechanism. 11 Further, the values of ΔG^{0} became more negative with raise in temperature, suggesting that the 12 adsorption is more favorable at higher temperatures. Positive value (+1.46kJ/mol) of ΔH^0 13 suggested the endothermic nature of removal process which indicates that higher removal can be 14 achieved at elevated temperature. Determination of ΔS^{0} is helpful for describing the randomness 15 16 at the solid/solution interface during the adsorption process. Further, positive value (+1491 J $\text{mol}^{-1}\text{K}^{-1}$) of ΔS^0 showed increased randomness at the solid/solution interface during the 17 adsorption of dyes onto nanoparticles. The positive value of ΔS° for the TZ adsorption suggested 18 higher degree of freedom of the TZ molecules with the increase of the solution temperature. 19

20 Sticking probability (S*) and activation energy were also calculated by using modified Arrhenius

21 type equation²⁴:

22
$$S^* = (1 - \theta)e^{-Ea/RT}$$
 (15)

- 1 The S* is a function of the adsorbate/adsorbent system which is dependent on the temperature of
- 2 the system and the value of S^* lies in the range $0 \le S^* \le 1$. E_a is activation energy and calculated
- 3 from the slope of the plot of $\ln (1 \theta)$ versus 1/T. The value of θ can be calculated from the
- 4 following equation:

$$5 \theta = \left[1 - \frac{c_e}{c_0}\right] (16)$$

- 6 The value of activation energy gives an idea about the nature of adsorption process. In case of
- 7 involvement of physical adsorption, activation energy lies in the range of 5–40 kJ/mol while for
- 8 chemical adsorption, the values vary from 40–800 kJ/mol. The value of E_a for present system was
- 9 found to be 26.97 kJ/mol suggesting that physisorption is the predominant mechanism which is
- involved in TZ adsorption. Value of sticking probability was determined to be 2.3X10⁻⁴.

11 6. Isotherm modelling

- 12 Equilibrium adsorption isotherm represents the relation between concentration of adsorbate in the
- 13 liquid phase and on the adsorbent surface. Adsorption isotherm is also helpful to describe
- 14 interaction between adsorbent surface/adsorbate species and determine the maximum adsorption
- capacity³². For obtaining equilibrium data, experiments were carried out with different dye
- 16 concentrations (100 to 200mg/L) at different temperatures. Several isotherm models viz.
- 17 Langmuir, Freundlich, Redlich-Peterson, Dubinin-Radushkevich and Sips isotherm model were
- applied on the equilibrium data.
- 19 *6.1. Langmuir isotherm model*
- 20 According to Langmuir isotherm, adsorption takes place at specific sites on the adsorbent surface
- and the adsorption energy is homogeneously distributed on the adsorbent surface³³. Molecular
- 22 interaction is not possible between adsorbed molecular species. The Langmuir isotherm can be
- expressed as follows:

- $1 q_e = \frac{q_m b C_e}{(1 + b C_e)} (17)$
- Where q_m (mg/g) is the maximum adsorption capacity of PPy@TN nanoparticles and b is the
- 3 Langmuir constant (L/ mg). $C_e(mg/L)$ and $q_e(mg/g)$ are the equilibrium concentration of dye
- 4 and adsorption capacity of nanoparticles at equilibrium respectively.
- 5 **Fig.11**
- 6 *6.2. Freundlich isotherm model*
- 7 Freundlich isotherm assumes heterogeneous distribution of active sites and also supports for
- 8 multilayer adsorption³⁴. According to Freundlich isotherm interactions are possible between
- 9 adsorbed molecules. The Freundlich isotherm model is represented by following equation:

10
$$q_e = K_f C^{\frac{1}{n}}$$
 (18)

- Where K_f (mg/g (L/mg)^{1/n}) and 1/n are Freundlich constants related with adsorption capacity and
- the heterogeneity factor. Value of 1/n gives an idea about the type of isotherm to be irreversible
- 13 (1/n=0), favorable (0</n<1) and unfavorable (1/n>1).
- 14 6.3. Dubinin and Radushkevich isotherm model
- Dubinin and Radushkevich isotherm are helpful in the determination of adsorption energy and 30
- can be expressed as follows³⁵:

$$17 q_e = q_m \exp(-\beta \varepsilon^2) (19)$$

18
$$\varepsilon = RT ln \left(1 + \frac{1}{C_e} \right)$$
 (20)

$$19 E = \frac{1}{\sqrt{2\beta}} (21)$$

- Where q_m is the maximum adsorption capacity (mg/g); R is the gas constant (8.314 J/mol K); T is
- 21 the absolute temperature and constant β (mol² kJ⁻²) gives the mean free energy. ϵ is the Polanyi

- potential and E is related to the mean free energy of the adsorption per mole of the adsorbate
- 2 (kJ/mol).
- 3 *6.4. Sips isotherm*
- 4 The Sips isotherm is a combination of Langmuir and Freundlich isotherm and can be expressed as
- 5 follows:

6
$$q_e = \frac{q_m (K_s C_e)^{m_S}}{1 + (K_s C_e)^{m_S}}$$
 (22)

- 7 Where q_m is the Sips maximum adsorption capacity (mg/g), K_S is the Sips equilibrium constant
- 8 (L/mg), and m_s is the Sips model exponent. In case of low adsorbate concentrations, it reduces to
- 9 Freundlich isotherm while for high adsorbate concentrations, it behaves like Langmuir isotherm³⁶.
- 10 6.5. Redlich–Peterson isotherm
- 11 The Redlich-Peterson isotherm can be applied for both homogeneous and heterogeneous
- systems³⁷. The Redlich–Peterson isotherm can be represented by the following equation:

$$13 q_e = \frac{k_{rp}c_e}{1 + a_{rp}c_e^{\beta}} (23)$$

- Where k_{RP} and a_{RP} are the Redlich-Peterson constants (L/g) and (L/mg) and β an exponent that
- lies between 0 and 1. The isotherm parameters were determined by nonlinear regression, using the
- Microsoft excel solver 2010. The coefficient of determination r² helps in the determination of
- best fit isotherm model which was calculated from the following equation³⁸:

18
$$r^2 = \frac{\sum (q_m - \overline{q_e})^2}{\sum (q_m - \overline{q_e})^2 + \sum (q_m - q_e)^2}$$
 (24)

- where q_e is the equilibrium adsorption capacity determined by experiments, q_m is the isotherm
- 20 predicted equilibrium adsorption capacity. The nonlinear isotherm plots for different isotherms are
- shown in Figs.11a,b,c,d and the parameters calculated for different isotherm models are

- summarized in Table 2. χ^2 value was determined for different isotherms to predict best model
- 2 among all studied isotherms by using following equation²⁵.

3 The Chi square
$$\chi^2 = \sum \frac{(q_{e,exp} - q_{e,cal})^2}{q_{e,cal}}$$
 (25)

- Where $q_{e,exp}$ and $q_{e,cal}$ are the equilibrium capacity calculated from experiments and calculated by
- 5 isotherm model respectively. On comparing r^2 and χ^2 values for all isotherms, Redlich-
- 6 Peterson(R-P) isotherm was found to be best fit isotherm model for describing TZ adsorption on
- 7 PPy@TN nanoparticles.
- 8 Table. 2

11

12

13

14

15

16

17

18

19

20

21

22

9 7. Comparative study

Comparative study for the removal efficiency of polypyrrole coated nanoparticles with other available adsorbent materials for tartrazine was also carried out. Adsorption capacity of bottom ash and De-oiled ash for tartrazine dye was determined to be 2.358X10⁻⁵ and 4.608X10⁻⁵mol/g respectively¹⁰. In another study, hen feather was used as an adsorbent material for the removal of tartrazine and its adsorption capacity was observed to be 0.00014 (mol/g)⁶. Banerjee and Chattopadhyaya (2013) investigated efficiency of saw dust for tartrazine dye³⁹. Langmuir adsorption capacity of saw dust was determined to be 4.71mg/g. Further carbon nanotubes decorated with silver nanoparticles were synthesized for tartrazine removal and it was found very efficient for the tartrazine adsorption (85.09mg/g)⁹. Adsorption capacity of commercial activated carbon(CAC), coconut shell activated carbon(CSAC) and *Lantana* carbon was reported to be 4.484, 2.257 and 90.9mg/g respectively^{40,41}. In another study polyaniline nanolayer composite was synthesized by Ansari et al. ⁴². Adsorption capacity of polyaniline nanolayer composite was found to be 2.47mg/g. It is clear from comparative study that the adsorption capacity of synthesized

- 1 polypyrrole coated tenorite nanoparticle (42.50mg/g) is quite comparable with the other available
- 2 adsorbent materials.

7. Metal removal from synthetic wastewater

- 4 In the present study, tartrazine dye loaded adsorbent (TZ-PPY@TN) was used as an adsorbent
- 5 material for the removal of Co(II), Mn(II), Pb(II), Cd(II) and Zn(II) metals from single and
- 6 multisolute system.

7 Fig.12

- 8 Tartrazine dye loaded on nanoparticles acts as modifying agent which makes nanoparticles
- 9 surface suitable for metal adsorption⁴³. Adsorption capacity of TZ loaded nanoparticles (TZ-
- 10 PPY@TN) for different metals is shown in Fig 12. It can be observed in Fig 12 that a wide range
- of metal concentrations can be efficiently treated with TZ loaded nanoparticles. Following trend
- was observed in the single solute system.

13 $\operatorname{Co}(II) < \operatorname{Mn}(II) < \operatorname{Pb}(II) < \operatorname{Cd}(II) < \operatorname{Zn}(II)$

- A similar trend was also observed in case of multi-solute metal solution of these metallic species.
- Adsorption of different metallic species depends on different factors viz. speciation of metallic
- species, degree of ionization etc. Detailed study is recommended for complete illustration of
- metal-TZ loaded nanoparticle interaction.

18 8. Conclusions

- 19 Following conclusions may be drawn from the present study.
- 20 i. Polypyrrole coated tenorite nanoparticles with 30 nm diameter and 425 m^2/g BET surface
- area were successfully synthesized.

- 1 ii. TEM images showed the formation of brick like structure in Polypyrrole coated tenorite
- 2 nanoparticles.
- 3 iii. Synthesized nanoparticles were found to be very efficient for the removal of dye in all the
- 4 selected concentration ranges.
- 5 iv. pH study reveals that maximum removal can be achieved at 2.0 pH as adsorbent surface
- supports dye anion adsorption due to positively charged surface in acidic medium.
- v. Dye removal increased on increasing the temperature, which shows endothermic nature of
- 8 the removal process.
- 9 vi. The negative value of ΔG^0 at all temperatures suggest the feasibility of tartrazine
- adsorption on polypyrrole coated tenorite nanoparticles.
- vii. Dye loaded nanoparticles were used as an efficient adsorbent for different metallic species
- from the single and multisolute system.
- 13 Present study indicates the versatile nature of the polypyrrole coated tenorite nanoparticles
- because it was found to be efficient for tartrazine dye as well as for metallic species which make it
- a strong candidate for the treatment of dye laden and metal bearing wastewater.

16 Acknowledgement

- 17 The authors are thankful to the Regional Council of South-Savo and the City of Mikkeli for
- 18 funding and Mikkeli *University of Applied Sciences* for providing SEM analysis of samples.

19 References

- 20 [1] A. Rodríguez, J. García, G.Ovejero and M. Mestanza, J. Hazard. Mater, 2009, 172, 1311-
- 21 1320.
- 22 [2] E. T. Acar, S. Ortaboy and G. Atun, *Chem. Eng. J.*, 2015, **276**, 340–348.
- 23 [3] S. J. Allen, G. Mckay and J. F. Porter, *J. Colloid Interface Sci.* 2004, **280**, 322–333.

- 1 [4] A. González, M. E. Villanueva, L. L. Piehl and G. J. Copello, *Chem. Eng. J.*, 2015, **280**, 41–48.
- 2 [5] G.L. Dotto, J.M. Moura, T.R.S. Cadaval, L.A.A. Pinto, *Chem. Eng. J.* 2013, **214**, 8.
- 3 [6] A. Mittal, L. Kurup, J. Mittal, *J. Hazard. Mater.* 2007, **146**(1–2),243.
- 4 [7] C. Klett, A. Barry, I. Balti, P. Lelli, F. Schoenstein and N. Jouini, *J. Environ. Chem. Eng.*,
- 5 2014, **2**, 914–926.
- 6 [8] M. Wawrzkiewicz, Z. Hubicki, J. Hazard. Mater. 2009, 164(2–3),502.
- 7 [9] J. Goscianska and R. Pietrzak, *Catalysis Today*, 2015, **249**, 259–264.
- 8 [10] A. Mittal, J. Mittal, L. Kurup, *J. Hazard. Mater.* 2006, **136**(3),567.
- 9 [11] W. Brostow, H.E. Hagg Lobland, S. Pal, R.P. Singh, J. Mater. Ed. 31,2009, 157.
- 10 [12] Á. Sánchez-Sánchez, F. Suárez-García, A. Martínez-Alonso and J. M. D. Tascón, J
- 11 *Colloid Interface. Sci.*, 2015, **450**, 91–100.
- 12 [13] H. Mittal, A. Maity, S.S. Ray, *Int. J. Biol. Macromol.* 2015, 79, 8.
- 13 [14] G. Akkaya Sayğılı, *J. Mol. Liq.*, 2015, **211**, 515–526.
- 14 [15] D.Ljubas, G.Smoljanic, H. Juretic, J. Environ Manage. 2015, **161**, 83-91.
- 15 [16] D.A.Giannakoudakis, G.Z.Kyzas, A.Avranas ,N. K. Lazaridis, J. Mol. Liq., 2015
- 16 [17] F.Motahari, M.R. Mozdianfard, M.Salavati-Niasari, Process Saf. *Environ. Prot.* 2015, **93**
- 17 ,282.
- 18 [18] L. Lian, X. Cao, Y. Wu, D. Lou, D. Han, *J. Taiwan Inst. Chem. Eng.* 2013,44(1),67.
- 19 [19] S. Mohammadi, G. Khayatian, Spectrochim. Acta. A.Mol. Biomol. Spectrosc. 148, 2015
- 20 405.
- 21 [20] S. Dadfarnia, A.M. Haji Shabani, S.E. Moradi, S. Emami, Appl. Surf. Sci. 2015, 330, 85.
- 22 [21] E. Tahmasebi, Y. Yamini, S. Seidi, M. Rezazadeh, *J. Chromatogr. A* 2013, **1314**, 15–23.

- 1 [22] M.B. Gholivand, Y. Yamini, M. Dayeni, S. Seidi, E. Tahmasebi, J. Environ. Chem. Eng.
- 2 2015,**3**(1),529.
- 3 [23] S. Yadav, V. Srivastava, S. Banerjee, C.H. Weng, Y.C. Sharma, *Catena*. 2013,**100**,120.
- 4 [24] N.M. Mahmoodi, B. Hayati, M. Arami, H. Bahrami, *Desalination*. 2011, **275**(1–3) 93.
- 5 [25] T.G. Venkatesha, Y.A. Nayaka, B.K. Chethana, *Appl. Surf. Sci.* 2013, **276**,620.
- 6 [26] V. Srivastava, Y.C. Sharma, M. Sillanpää, *Appl. Surf. Sci.* 2015, **338**,42.
- 7 [27] W. J. Weber and J. C. Morris, *J. Sanit. Eng. Div.*, 1963, **89**, 31.
- 8 [28] G. E. Boyd, A. W. Adamson and L. S. Myers, J. Am. Chem. Soc., 1947, **69**, 2836–2848
- 9 [29] D. H. Bangham and F. P. Burt, Proceedings of the Royal Society of London A:
- 10 *Mathematical, Phy. Eng. Sci.*, 1924, **105**, 481–488.
- 11 [30] V.S. Mane, I. Deo Mall, V. Chandra Srivastava, *J. Environ. Manage.* 2007, **84**(4) 390
- 12 [31] M. Ghaedi, B. Sadeghian, A.A. Pebdani, R. Sahraei, A. Daneshfar, C. Duran, *Chem. Eng.*
- *J.* 2012,**187**,133.
- 14 [32] S. Zeng, S. Duan, R. Tang, L. Li, C. Liu, D. Sun, *Chem. Eng. J.* 2014, **258**,218.
- 15 [33] R. Chen, W. Wang, X. Zhao, Y. Zhang, S. Wu, F. Li, *Chem. Eng. J.* 2014, **242**,226.
- 16 [34] I. Langmuir, J. Am. Chem. Soc., 1916, 38, 2221–2295.
- 17 [35] Freundlich, H.M.F. J. Phys. Chem. **1906**, 57, 385–471.
- 18 [36] M.M. Dubinin, L.V. Radushkevich, Proc. Acad. Sci. USSR Phys. Chem. Sect.
- 19 1947,55,331–337.
- 20 [37] T. Madrakian, A. Afkhami, M. Ahmadi, Spectrochim. Acta. A. Mol. *Biomol. Spectrosc.*
- 21 2012, **99**,102.
- 22 [38] O. Redlich, D.L. Peterson, J. Phys. Chem. 1959 63(6),1024.
- 23 [39] Y.S. Ho, *Pol.J.Environ.Stud.*2006, **15**(1)81.

- 1 [40] S. Banerjee, M.C. Chattopadhyaya, Arabian J. Chem.2013, 10.1016/j.arabjc.2013.06.005
- 2 [41] M. Jibril, J. Noraini, L. S. Poh and A. M. Evuti, *J. Teknol.*, 2013, **60**, 15.
- 3 [42] R.K. Gautam, P.K. Gautam, S. Banerjee, V. Rawat, S. Soni, S.K. Sharma, M.C.
- 4 Chattopadhyaya, J. Environ. Chem. Eng. 2015,3(1),79.
- 5 [43] R. Ansari, M.B. Keivani, A.F. Delavar, J. Polym. Res. 2011, 18 (6), 1931.
- 6 [44] L. Monser, N. Adhoum, J. Hazard. Mater. 2009, **161**(1), 263

4 Table 1. The values of different kinetic parameters for the removal of TZ by PPy@TN

5 nanoparticles.

	Concentration	Experimental	Predicted q _e	k ₁ x10 ⁻⁶ (min ⁻¹)	\mathbb{R}^2
	of dye solution	$q_e(mg/g)$	(mg/g)	,	
Pseudo first	125 mg/L	32.60	6.53	7.8	0.93
order kinetic	150 mg/L	35.98	7.12	7.1	0.99
parameters	175 mg/L	38.34	10.49	7.5	0.95
	200 mg/L	41.28	13.20	8.7	0.96
		Experimental	Predicted q _e	k ₂ x ₁₀ -7	R^2
Pseudo		$q_e(mg/g)$	(mg/g)	$(g mg^{-1} min^{-1})$	
second order					
kinetic parameters	125 mg/L	32.60	32.05	0.56	0.99
	150 mg/L	35.98	35.21	0.53	0.99
	175 mg/L	38.34	37.31	0.33	0.99
	200 mg/L	41.28	40.65	0.24	0.99
		C(mg/g)	k _{id}	R^2	
Inraparticle					
diffusion	125 mg/L	25.48	0.39	0.97	
parameters	150 mg/L	27.72	0.46	0.97	
	175 mg/L	26.85	0.63	0.98	
	200 mg/L	27.17	0.81	0.98	
		B(min ⁻¹)	Di x10 ⁻¹⁸	R^2	
		,	(m^2/min)		
Boyd model parameters	125 mg/L	0.0079	2.68	0.93	
	150 mg/L	0.0072	2.45	0.99	
	175 mg/L	0.0075	2.72	0.95	
	200 mg/L	0.0086	3.09	0.96	
		β(g/mg.min)	α(mg/g.min)	R^2	
Bangham		,			
model	125 mg/L	3.85	0.14	0.94	
parameters	150 mg/L	3.33	0.12	0.99	
	175 mg/L	2.46	0.13	0.95	
	200 mg/L	2.01	0.15	0.95	

Table. 2 Values of different isotherm parameters for TZ removal by PPy@TN nanoparticles.

	Langmuir	isotherm parameter	rs	
	25 ⁰ C	30^{0} C	35 ⁰ C	45 ⁰ C
$q_0(mg/g)$	38.21	39.73	40.63	42.50
b(L/mg)	1.24	2.18	3.49	9.09
r^2	0.67	0.61	0.60	0.55
χ^2	0.81	1.33	1.55	2.49
	Freundlich	isotherm paramete	rs	
$K_f(mg^{1-1/n}L^{1/n}g^{-1})$	25.69	27.41	28.99	31.80
n (g/L)	9.52	9.43	9.82	10.11
R^2	0.91	0.88	0.87	0.82
χ^2	0.22	0.46	0.53	1.09
Dubin	in–Radushkev	ich (D –R) isotherr	n parameters	
q _m (mg/g)	37.18	38.96	40.04	42.18
$\beta (\text{mol}^2/\text{kJ}^2)$	1.97	0.79	0.40	0.13
E(kJ/ mol),	0.50	0.79	1.11	1.93
r ²	0.56	0.54	0.55	0.52
χ^2	1.03	1.54	1.74	2.62
Re	dlich–Peterson	(R-P) isotherm pa	rameters	
$A_{rp}(L/g)$	0.16	0.24	0.26	0.48
$B_{rp}(L/g)$	28.27	29.14	29.73	30.34
g	0.024	0.019	0.027	0.013
$\frac{g}{r^2}$	0.99	0.99	0.98	0.99
χ^2	0.01	0.02	0.04	0.04
	Sips Iso	otherm parameters		
q _m (mg/g)	19.49	20.05	22.55	25.97
K _S (L/mg)	8.63	12.08	7.69	5.29
m_s	0.104	0.106	0.101	0.098
r ²	0.91	0.87	0.88	0.82
χ^2	0.22	0.46	0.53	1.09

4

3

Caption of figures

- 5 Fig.1 Structure of tartrazine dye⁹.
- 6 Fig. 2 XRD of (a) nano tenorite; (b) polypyrrole coated tenorite nanoparticles (PPy@TN);(c)
- 7 tartrazine loaded nanoparticles (TZ-PPy@ TN); (a-1) EDS of nano tenorite; (b-1) polypyrrole
- 8 coated tenorite nanoparticles (PPv@TN);(c-1) tartrazine loaded nanoparticles (TZ-PPv@TN).

9

- Fig.3 (a and b) TEM of nano tenorite; (c and d) PPy@TN and (e and f) TZ-PPy@TN.
- Fig.4 (a and b) SEM of of nano tenorite; (c and d) PPy@TN; (e and f) TZ-PPy@TN.
- Fig. 5 Nitrogen adsorption-desorption isotherm plot for PPy@TN nanoparticles.
- Fig. 6 Effect of initial concentration on dye removal.
- Fig. 7(a) Effect of pH on removal of TZ from synthetic wastewater(b) pH_{zpc} of PPy@TN
- 15 nanoparticles.

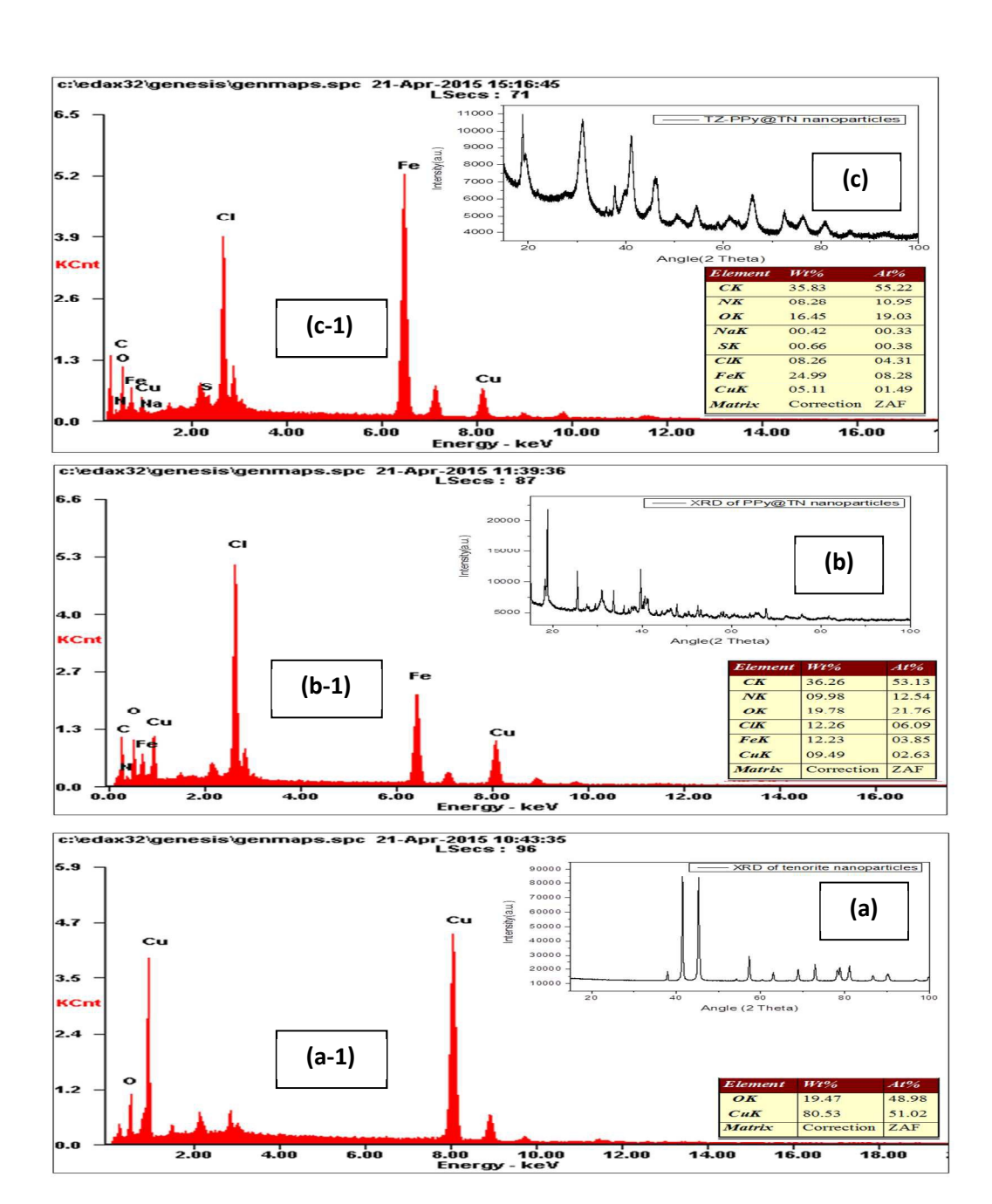
16

- Fig. 7b Effect of solution pH on adsorbent surface.
- Fig. 8 Effect of adsorbent dose on TZ removal from synthetic wastewater.
- 19 Fig.9. (a) Pseudo first order plot (b) pseudo second order kinetic plot for TZ adsorption by
- 20 PPy@TN nanoparticles.
- 21 Fig.10. (a) Intraparticle diffusion plot (b) Boyd plot (c) Bangham plot for TZ adsorption by
- 22 PPy@TN nanoparticles.
- Fig.11 Effect of temperature on removal of TZ from synthetic wastewater.
- 24 Fig. 12 Nonlinear isotherm plot for the adsorption of Tartrazine on nanoparticles (a) 293K; (b)
- 25 303 K; (c)313 K; (d) 323K.

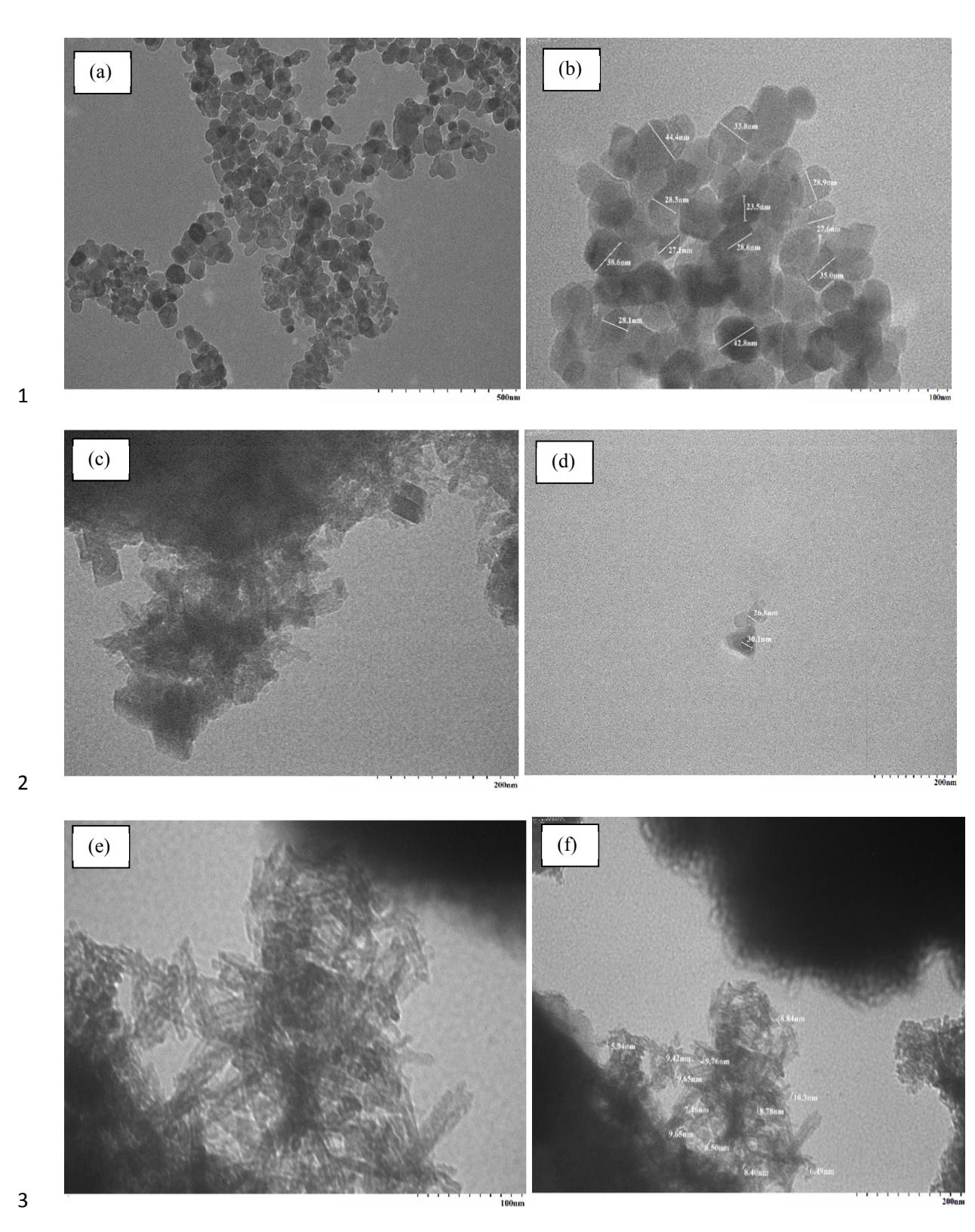
26

27 Fig.13 Removal of metals from single solute and multisolute synthetic wastewater.

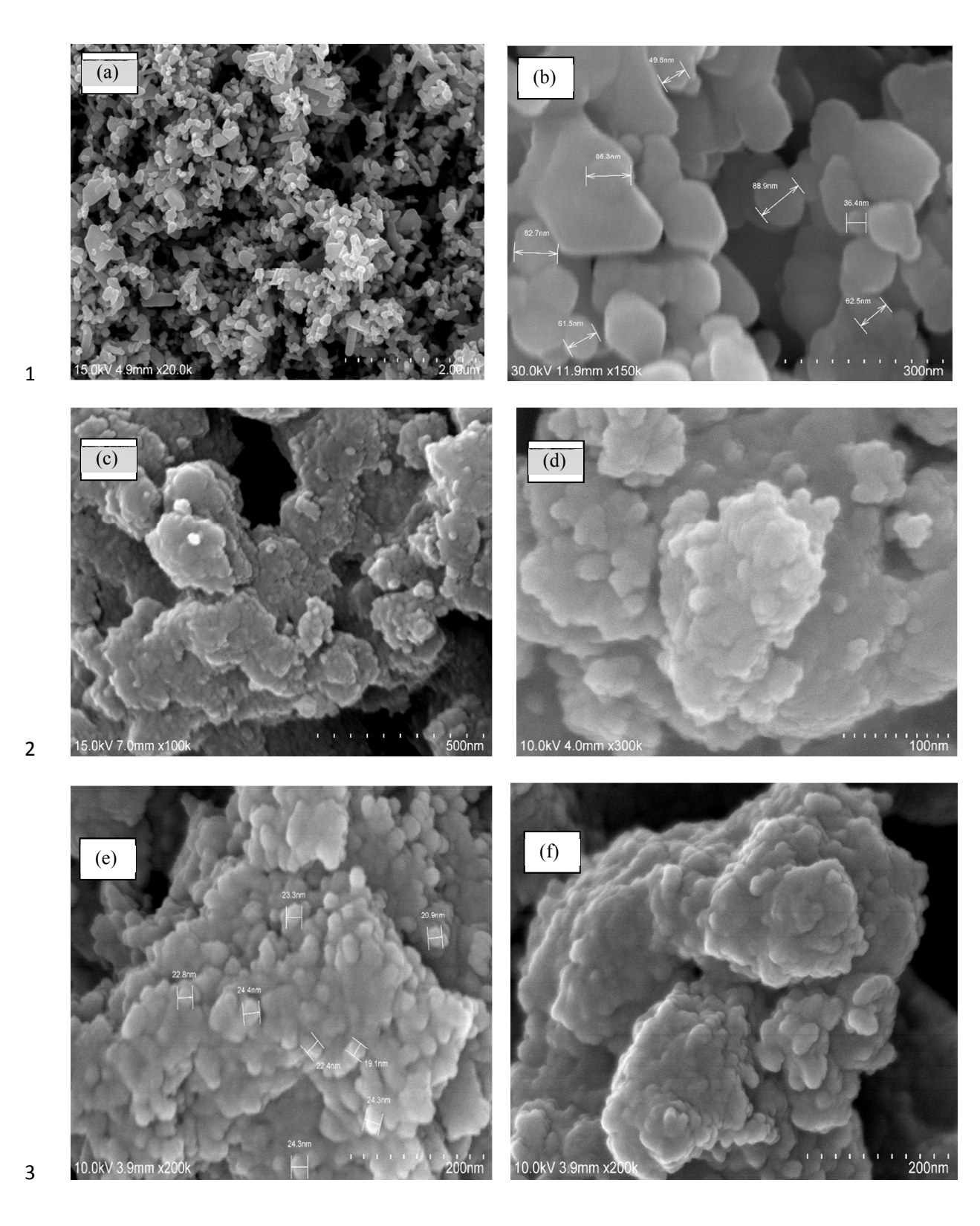
6 Fig.1



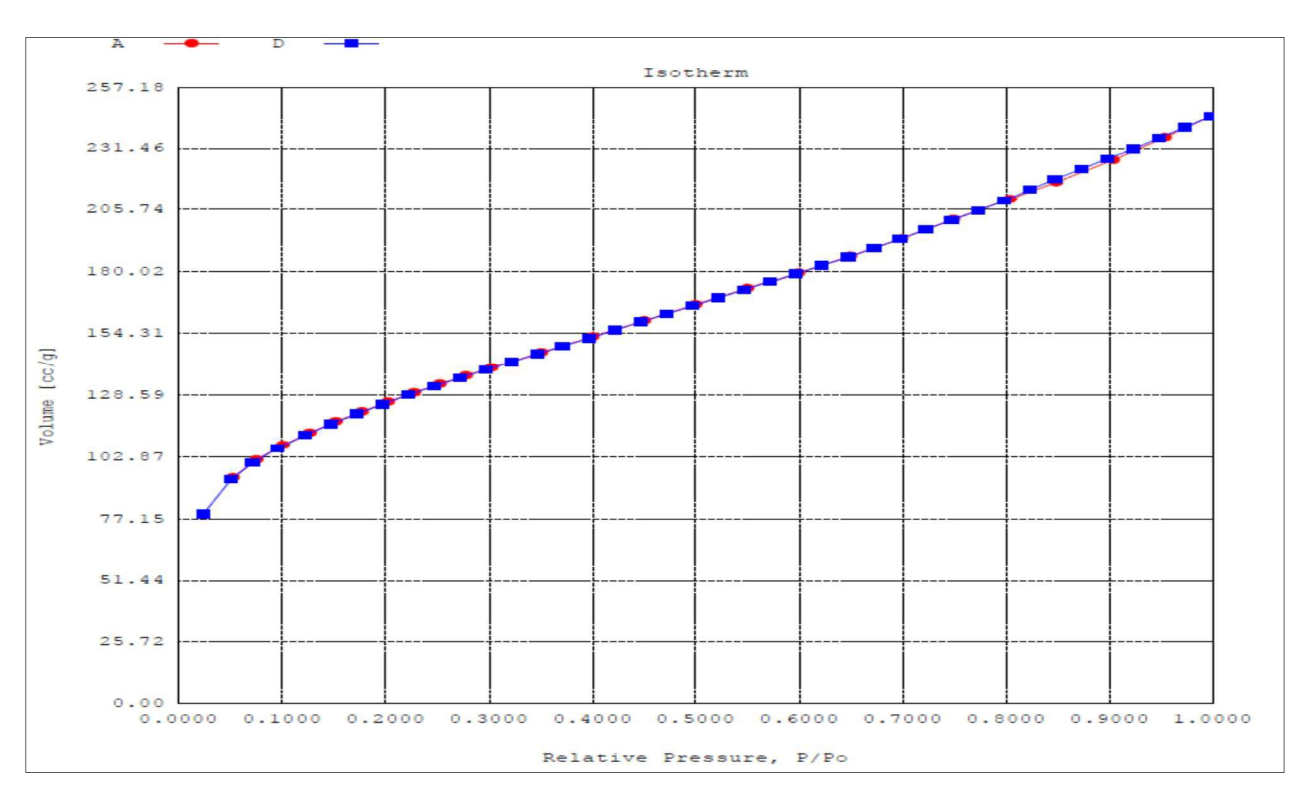
2 Fig. 2



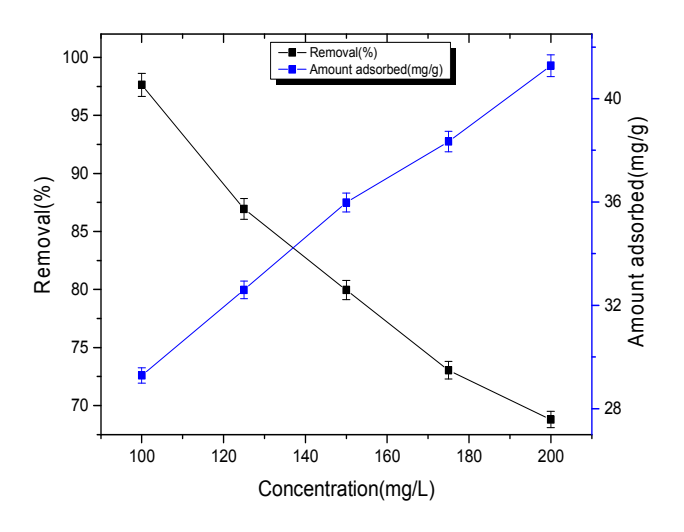
4 Fig.3



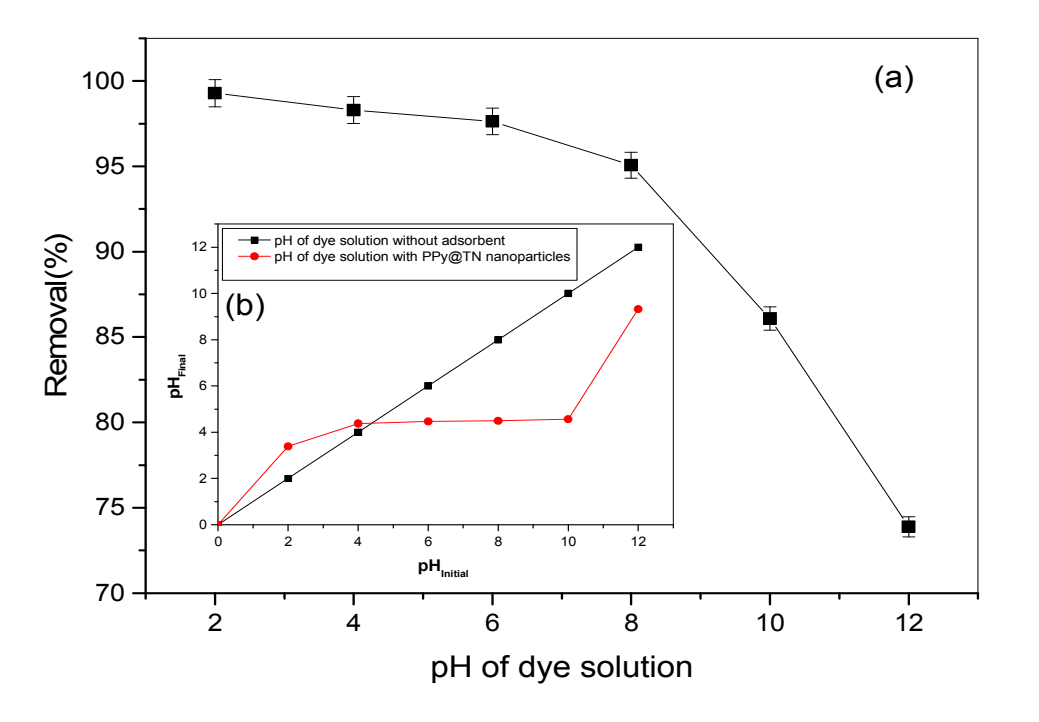
4 Fig.4



3 Fig. 5



2 Fig. 6

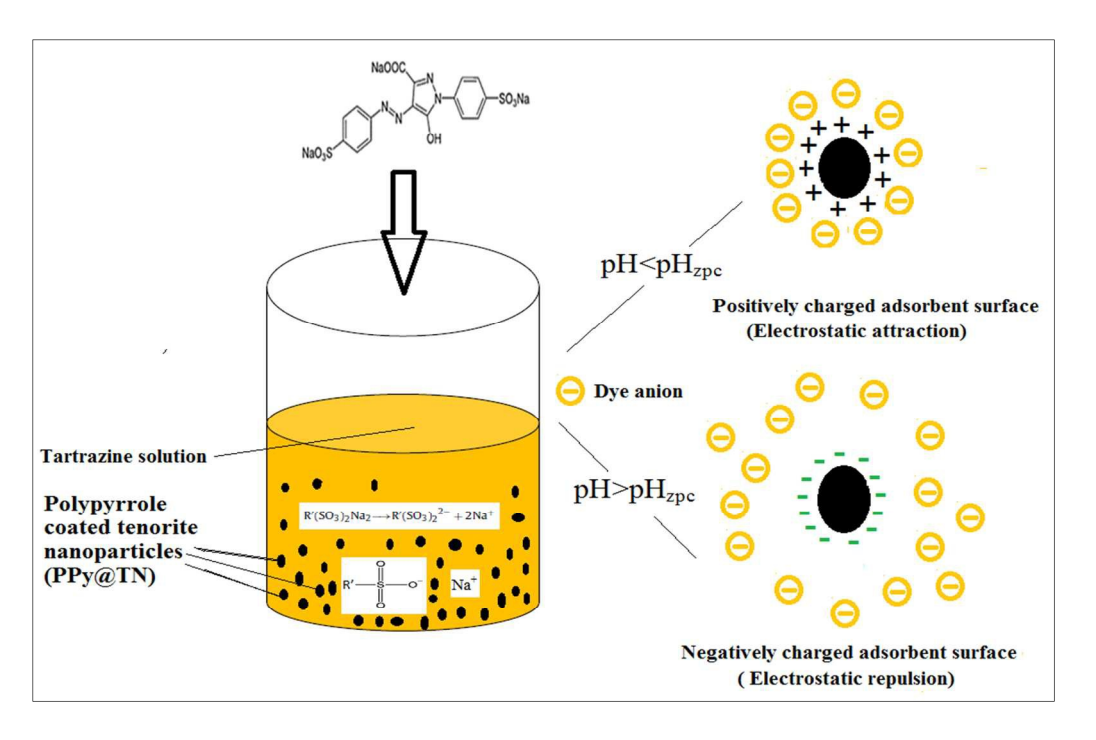


1 .

2 Fig.7(a)

3

4

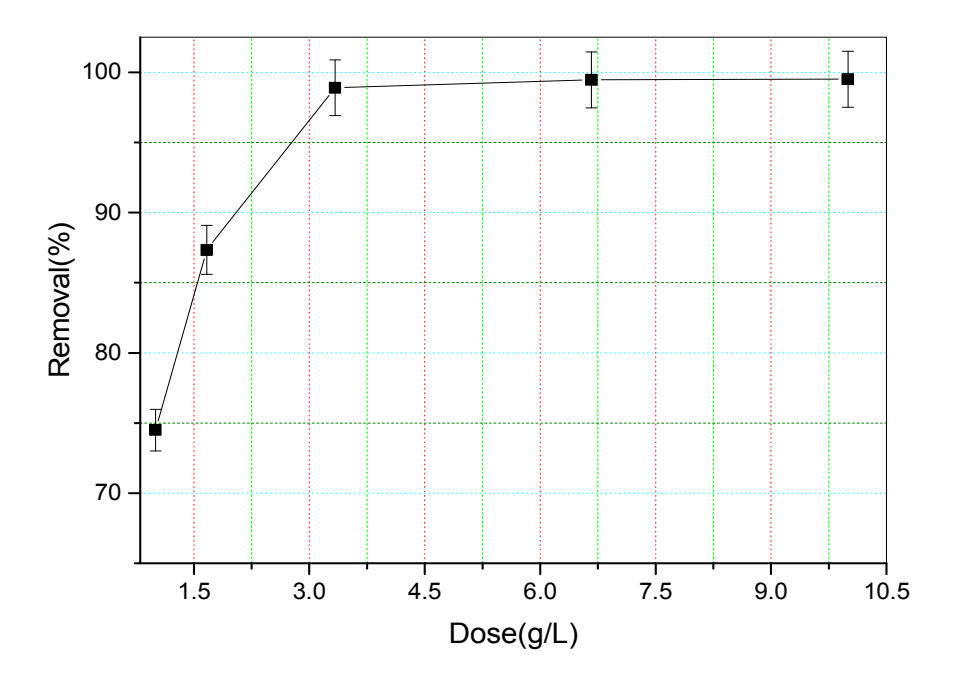


2 Fig. 7b

4

5

3



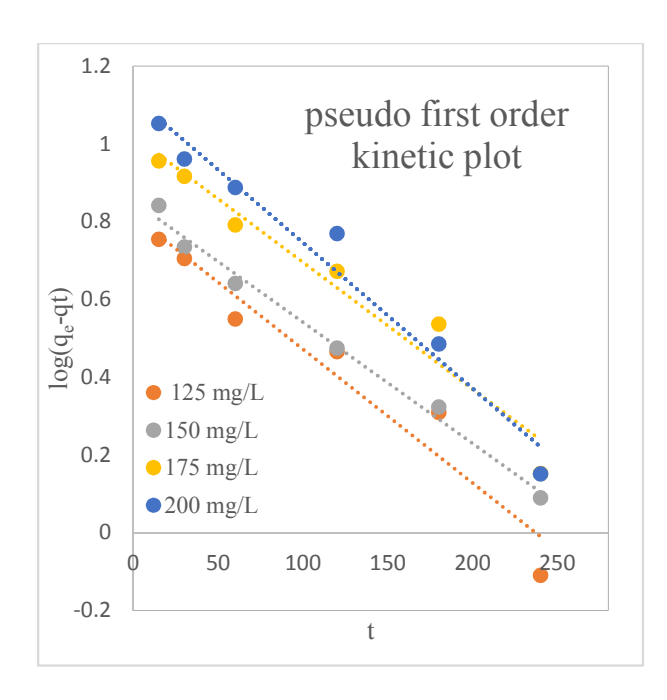
2 Fig.8

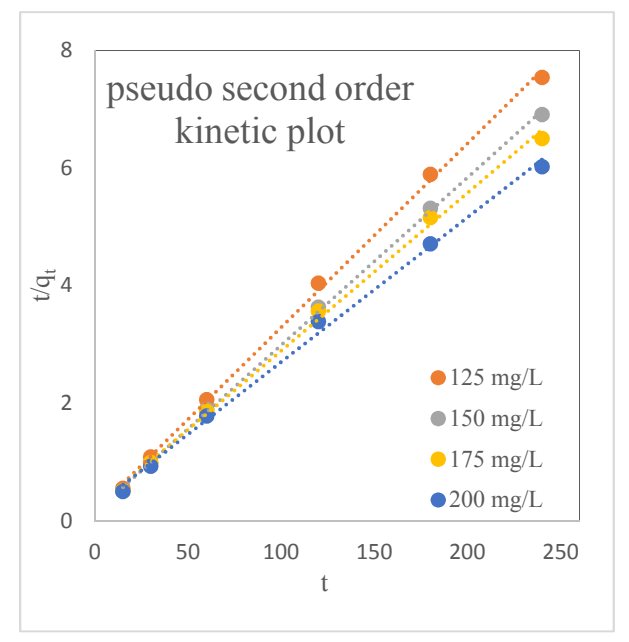
3

1

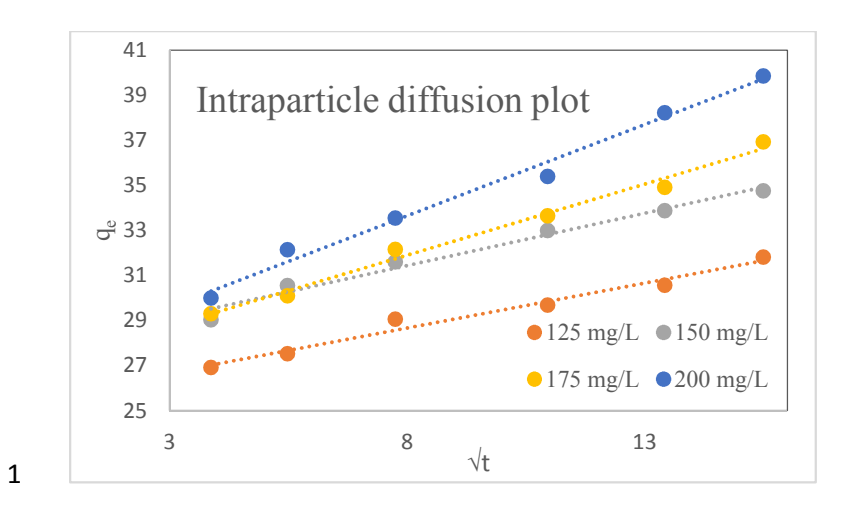
4

5

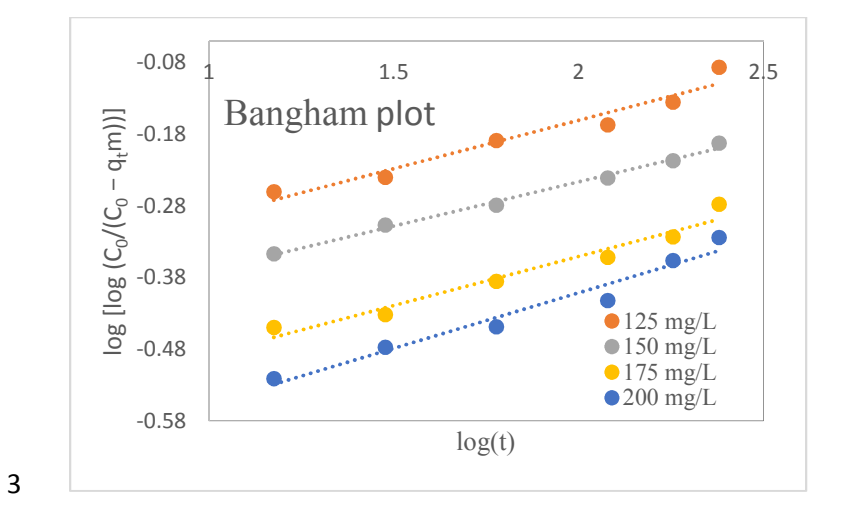




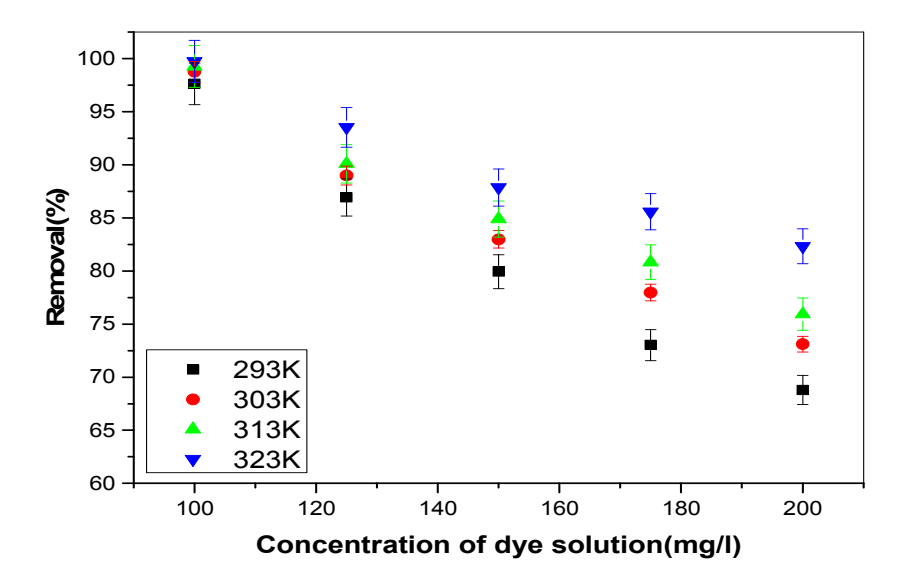
2 Fig.9.



3.5 Boyd plot 3 2.5 2 Bt 1.5 ●125 mg/L 1 ● 150 mg/L ● 175 mg/L 0.5 ●200 mg/L 0 100 0 50 150 200 250 t



4 Fig.10.

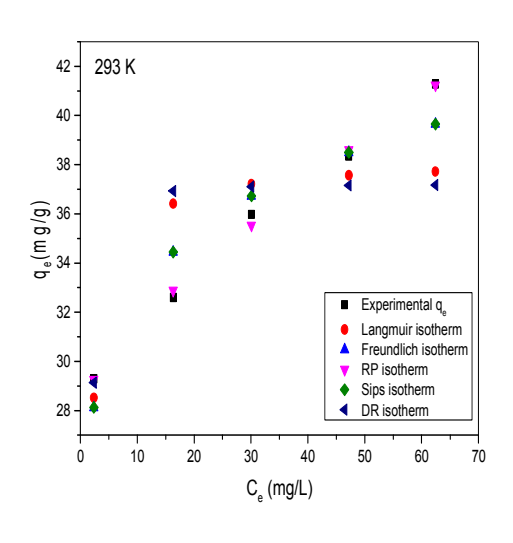


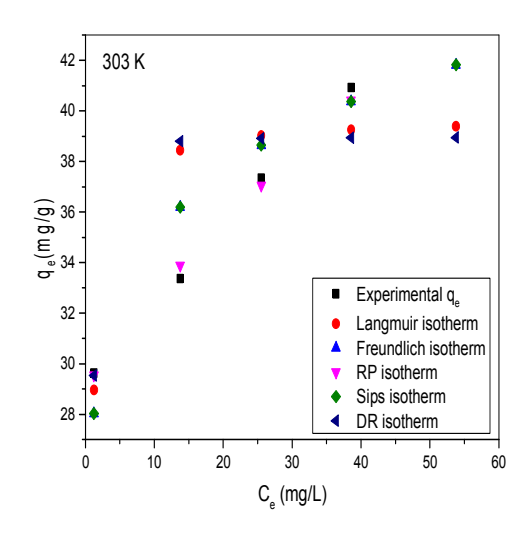
2 Fig.11

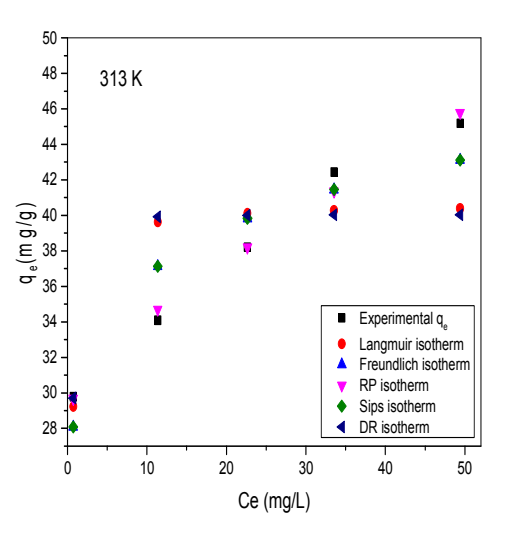
3

1

4







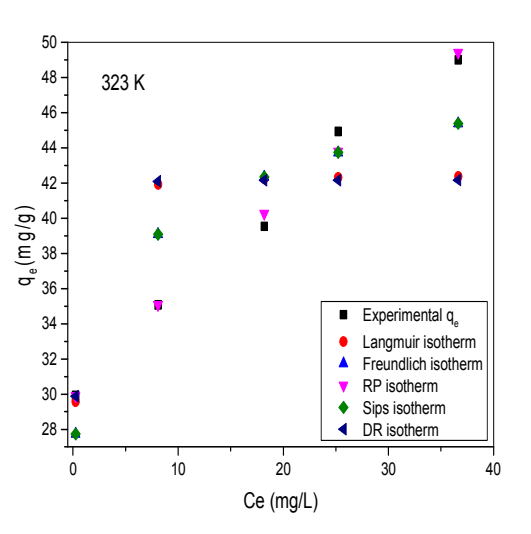
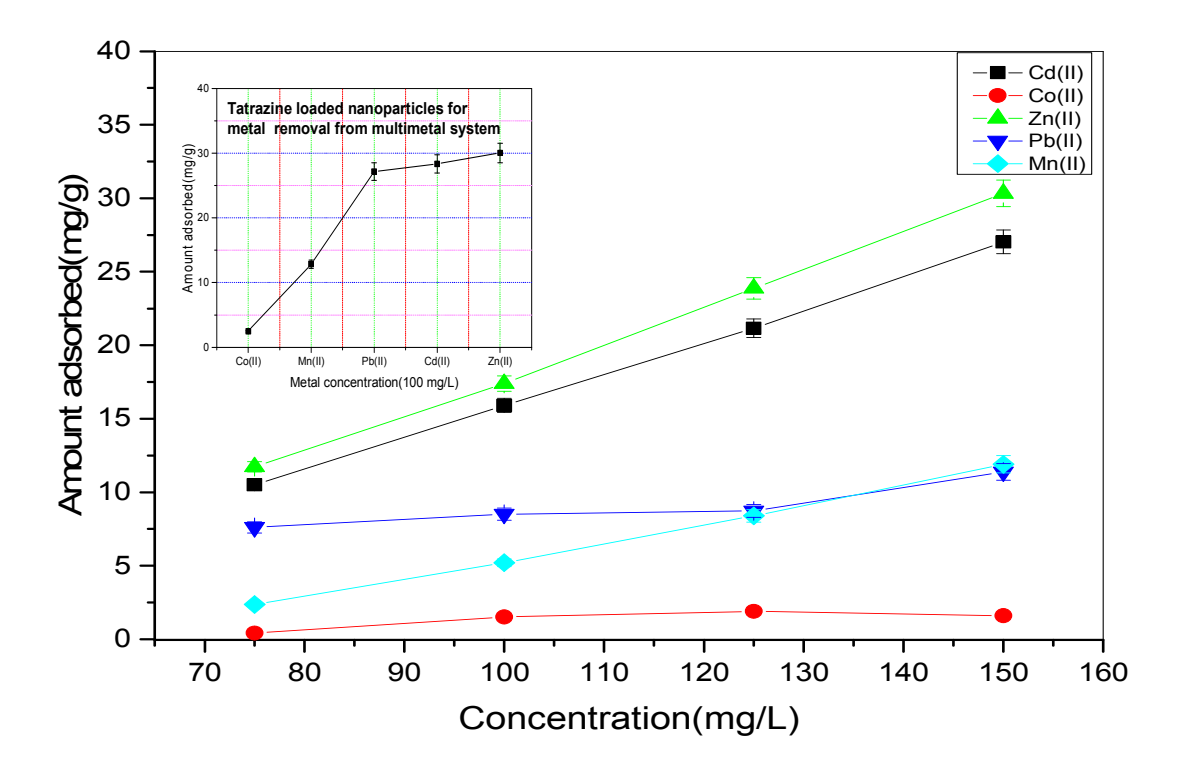


Fig.12



1 Fig.13

3

4

5

6

Graphical abstract

